30th Annual International IEEE EMBS Conference
Vancouver, British Columbia, Canada, August 20-24, 2008

A Deformable Model-Based System for 3D Analysis and Visualization of Tumor in PET/CT Images

Jérôme Landré, Stéphane Lebonvallet, Su Ruan, Li Xiaobing, Qiu Tianshuang, François Brunotte

Abstract— **This paper presents a tumor detecting system that allows interactive 3D tumor visualization and tumor volume measurements. An improved level set method is proposed to automatically segment the tumor images slice by slice. PET images are used to detect the tumor while CT images make a 3D representation of the patient's body possible. An initial slice with a seed within the tumor is firstly chosen by the operator. The system then performs automatically the tumor volume segmentation that allows the clinician to visualize the tumor, to measure it and to evaluate the best medical treatment adapted to the patient.**

I. INTRODUCTION

PET (Positron Emission Tomography) and CT (Computed Tomography) scans are both standard imaging tools that physicians use to follow disease states in the body in one single examination. Registration between both images is not needed. A PET detects changes in cellular function: how cells are utilizing nutrients like sugar and oxygen. Since these functional changes take place before physical changes occur, PET can provide information that enables physician to make an early diagnosis. A CT scanner uses a combination of X-rays and computers to give the radiologist a non-invasive way to see the human anatomy such size, shape and location. One advantage of CT is its ability to rapidly acquire multiple two-dimensional image slices of the anatomy.

In summary, PET/CT combines the functional information from PET with the anatomical information from CT into one single examination. By combining these two scanning technologies, a PET/CT scan enables physicians to more accurately diagnose and identify cancer, heart disease and brain disorders and also to determine how much cancer has spread, and how well cancer treatment is working.

Many segmentation methods have already been used in the medical imaging field. Magnetic Resonance Images (MRI) have been widely used to detect cancer tumors [1], [2], [3], [4]. Among various image segmentation techniques, active contour model [5] has emerged as a powerful tool for semi-automatic object segmentation. The basic idea is to evolve a curve, subject to constraints from a given image, for detecting interesting objects in that image. It consists in the resolution of systems of partial differential equations for which interface propagation phenomenon has to be described. The active contour models are often implemented based on level set method [6], which is a powerful tool to capture deforming shape. But it has the disadvantage of a heavy computation requirement even using the narrow band evolution. The most common way to initialize the level set is the manual selection of a region of interest (ROI) which seems to be relevant [7], [8], [9]. To avoid heavy computation, an improved version of the level set algorithm is proposed.

The paper is organized as follows. Section II presents the level set method. Our improved algorithm is given in section III. Experiments are explained in section IV. A conclusion and some perspectives are proposed in section V.

Jérôme Landré, Stéphane Lebonvallet and Su Ruan are with CReSTIC, IUT de Troyes, 9 Rue de Québec, 10026 Troyes Cedex, France, phone: (+33)325427101, su.ruan@univ-reims.fr

XiaoBing Li and Tianshuang Qiu are with School of Electronic and Information Engineering, Dalian University of Technology, 116023, China

François Brunotte is with centre G.-F. Leclerc, University of Bourgogne, 1 rue professeur Marion, 21000 Dijon, France

II. ADAPTED LEVEL SETS

The level set method for capturing moving fronts was first introduced by Osher and Sethian [10] in 1988. Over these years, it has been used in a wide variety of fields including graphics, image processing and many others. An important application is image segmentation, in which the level set is initialized by an initial curve, evolves under an image related speed, stops at the object boundary under some criteria.

The level set with stopping edges model by Malladi et al. [11] can be shortly described as follows: Let Ω be a bounded open subset of R^2, define an image u_0 as, $u_0 : \Omega \rightarrow R$ and suppose C is a close curve evolving in Ω. Chan and Vese [12] proposed that if we run the evolution by minimizing the energy equation (1), then the curve will eventually stop at the object boundary.

$$\begin{aligned} E(C, c_1, c_2) = \quad & \mu.length(C) + \nu.area(inside(C)) \\ & + \lambda_1 \int_{in(C)} |u_0(x,y) - c_1|^2 dxdy \\ & + \lambda_2 \int_{out(C)} |u_0(x,y) - c_2|^2 dxdy \end{aligned} \quad (1)$$

where $E(C, c_1, c_2)$ is the energy function, the positive $\mu, \nu, \lambda_1, \lambda_2$ are fixed parameters, $u_0(x, y)$ is the intensity of the image at the point $(x, y)$and the constant parameters c_1, c_2 are the average intensity of the image inside and outside the curve C respectively.

To solve equation 1, it must be transformed to level set formulation by substituting the curve C with the zero level set $\phi(x, y)$, and by using Heaviside function $H(z)$ and Dirac function $\delta(z)$ to extend the integral region in equation 1 from $inside(C)$ and $outside(C)$ to the whole region Ω. We obtain:

$$\begin{aligned} E(C, c_1, c_2) = \mu \int_\Omega \delta(\phi(x,y)) |\nabla \phi(x,y)|^2 dxdy \\ + \nu \int_\Omega H(\phi(x,y)) dxdy \end{aligned}$$

978-1-4244-1815-2/08/$25.00 ©2008 IEEE.

$$+\lambda_1 \int_{\Omega} |u_0(x,y) - c_1|^2 H(\phi(x,y))dxdy$$

$$+\lambda_2 \int_{\Omega} |u_0(x,y) - c_2|^2 (1 - H(\phi(x,y)))dxdy \quad (2)$$

where $c_1(\phi), c_2(\phi)$ are the average of u_0 in $\phi \geq 0$ $(inside(C))$ and $\phi < 0$ $(outside(C))$ respectively.

By parameterizing the descent direction, we can deduce the Euler-Lagrange partial differential equation, and we obtain the level set equation 3:

$$\begin{aligned} \frac{\partial \Phi}{\partial t} &= \delta(\Phi)[div(\frac{\nabla \Phi}{|\nabla \Phi|}) \\ &\quad -\nu - \lambda_1(u_0 - c_1)^2 + \lambda_2(u_0 - c_2)^2] \\ &= 0 \end{aligned} \quad (3)$$

Chan and Vese [12] gave the following discretization formulation 4 of the equation 3:

$$\begin{aligned} \frac{\phi_{i,j}^{n+1} - \phi_{i,j}^{n}}{\Delta t} = \quad & \delta_e(\phi_{i,j}^n)[\mu K - \nu \\ & -\lambda_1(u_{0,i,j} - c_1(\phi^n))^2 \\ & +\lambda_2(u_{0,i,j} - c_2(\phi^n))^2 \end{aligned} \quad (4)$$

where $\phi_{i,j}^n = \phi(x_i, y_j, n\Delta t)$ is the discretization approximation of $\phi(x,y,t)$ with $n \geq 0, \phi^0 = \phi_0$, and $K = div(\frac{\nabla \Phi}{|\nabla \Phi|})$ is the curvature of the evolving curve, it is also the divergence of the unit normal of the curve. This segmentation model can segment not only object with great gradient but also without edges.

III. IMPROVED LEVEL SETS METHOD

The proposed system can segment the tumor in PET/CT volumes almost automatically, only need one time confirmation of the operator. The process of tumor segmentation from PET volumes can be divided into three steps: a) Segmentation of a single slice of the volume, b) Segmentation of the whole volume and c) Segmentation slice by slice following time during the whole therapeutic treatment period.

A. Segmentation of a single slice

First, by hand, the center of the tumor is obtained by mouse clicking in the middle of the volume. The system then calculates the intensity of the tumor, and segments this first slice with our level set segmentation model [12]. We add our stopping criteria to control the evolution of the curve, make sure it stops in time at the right position, and thus find out the segmentation results, i.e., the boundary and the intensity of the tumor.

In order to stop the curve evolution in time at the right spots near the boundary, we add two stopping criteria: a) At each step of the evolution, i.e., each iteration of the level set, calculate the amount of the new pixels generated only by the last iteration, if there are four continuous times with zero amount pixels, it means the last four iterations have not evolved the curve at all. We consider that it is suitable to stop here, otherwise, even if the iteration continues, it is with little probability to evolve the curve any more. b) At the end of every iteration, we search in the new pixels generated in the last iteration for the highest intensity pixel, compare it to the intensity of the tumor, which we have obtained in the start first slice before segmentation, if the new generated pixels highest intensity is far below, e.g., 40% lower than the intensity of the tumor, it is suitable to stop here to avoid overmuch evolution.

B. Segmentation extending to the whole volume

After the segmentation in a single slice has been done, we extend the segmentation to the whole volume; this takes two segmentation groups in two directions in the volume respectively: one is the segmentation in the left direction, segment the slice one by one from the slice chosen above to the beginning slice in the volume, the other is the segmentation in the right direction, from the slice chosen above to the end of the volume. In the process of the two direction segmentations, if there is no tumor present in a slice in one direction, we should stop segmenting in this direction. To all the slices except the first one, the last slice segmentation results are used to initialize the segmentation of the current slice, giving the appropriate initial curve specified by its center, the seed.

1) Stopping at the foreside or the tail of the volume: In general, the tumor, if any, is most probably present in the middle of the volume. So it is advisable to stop at the last slice with tumor in a direction of the volume for the sake of great efficiency and speed. This is accomplished by the searching tactic. First, search the pixels in the current slice within the region bounded by the last slice segmentation results, calculate the average of the five pixels with highest intensity, then compare it to the intensity of the tumor, if the average is far below, e.g., 50% lower than the intensity of the tumor, there must be no potential tumor in the current slice in this region, and then the segmentation in this direction is over, otherwise we should make use of this region to find the seed of the current slice.

2) Seed from last slice: Again, search the tumor in the current slice within the region bounded by the last slice segmentation results, surely there are some points with the intensities around the intensity of the tumor. Then choose a higher intensity (denote it as HighLevelIntensity, which may be 80% of the highest intensity in the current slice), then cut off the intensity by HighLevelIntensity from all the pixels inside the boundary, that is to say, if the intensity is equal or larger than HighLevelIntensity, then subtract HighLevelIntensity from it, if the intensity is smaller than HighLevelIntensity, set it to zero, after this cut off, only pixels whose intensity are larger stay not to be zero, and they may be grouped in several connectivity regions, select the region with the largest area, and then compute the barycenter of this region, we use it as the seed of the curve evolution of the current slice.

After obtaining the center of the initial curve, we draw a small circle with the radius of 5 to set up the initial curve, segment the slice with corresponding algorithm. We should mention that, in our practice, the seed has a great influence

on the segmentation results, an improper seed may make a great departure from the segmentation results to the tumor boundary in some cases.

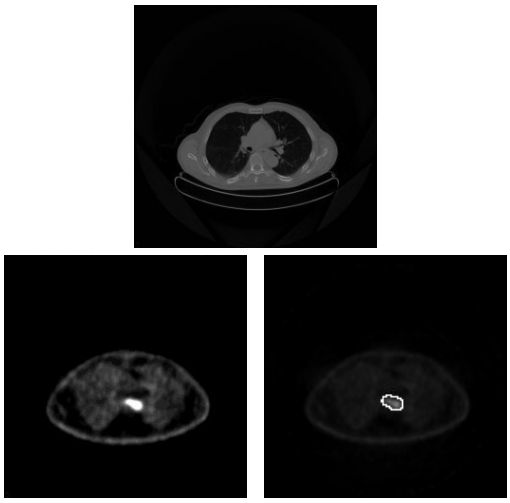

Fig. 1. A first example: CT1, PET1 and SEGM1 images.

We can see on figure 1 an example of CT slice (not used for segmentation), the corresponding PET slice and the result of the segmentation process on this PET slice.

IV. EXPERIMENTATION

A visualization tool has been developed in order to allow interactive tumor viewing in the patient's body. Our visualization tool is built under ImageJ [13], a free Java image processing program. ImageJ offers many image processing tools and the ability to extend basic methods by creating plugins that can be shared over the ImageJ community.

Let I_{CT} be the set of CT images representing slices of the body. Let I_{PET} be the set of PET images representing the result of the marked tumor. And let I_{SEGM} be the segmented images where the tumor has been detected. We have $I_{SEGM} \subset I_{PET}$ because segmentation is performed on PET images.

There are two problems to solve before combining PET and CT images : The resolution of PET and CT images are not the same and the spatial distance between PET and between CT slices are not the same.

The first problem to face is the difference of resolution of the images because of the difference of resolution of CT and PET sensors. CT images are 512×512 pixels 16-bits depth, PET images are 150×150 pixels 16-bits depth. As segmentation is performed on PET images and to avoid loss of information on these images, the resolution of CT images has been reduced to 256×256 pixels by a bilinear interpolation. Because combination of images needs same resolution images, PET images have been extended to 256×256 pixels with the same bilinear interpolation.

The spatial resolution of CT and PET sensors are not the same i.e. the step between two slices is not the same on I_{CT} and I_{PET}. In order to combine the two kind of images, a new stack of images has been created. Let s_{PET} be the step between PET images, let s_{CT} be the step between CT images. Because segmentation is performed on PET images, PET images were kept unchanged. In order to combine PET and CT images, virtual images have been created from CT real images to match the step distance.

In our case we have $s_{PET} = 4mm$ and $s_{CT} = 5mm$ so images to combine are not exactly in front of each other. On figure 2, virtual images p_0 and c_0 are combinable but there is a shift of one millimeter between p_4 and c_5. To fill the gap, a virtual image (represented in dots on the figure) c_4 is created. This image c_4 is built from c_0 and c_5, the previous and next image to the missing one. In order to take in consideration distance, the inter-distance between slices appears in the computation of our virtual image. c_4 is closer to c_5 (1 mm) than to c_0 (4 mm). So the expression of c_4 includes this proximity information. We have a weighted computation: $c_4 = (1 * c_0 + 4 * c_5)/5$.

Every virtual image needed for combination of PET and CT scans is computed with this weight information. For instance, $c_8 = (3 * c_{10} + 2 * c_5)/5$. This allows a better representation of slices of the body by solving the problem of the difference of spatial resolution between PET and CT sensors. So at the end, we have $r_0 = (p_0 + c_0)/2$, $r_4 = (p_4 + c_4)/2$ and so on with virtual images c_4, c_8, ...

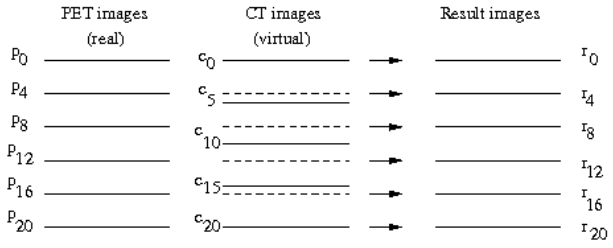

Fig. 2. Mixing slices with different steps (spatial resolutions).

From the fusion of images on figure 1, we obtain slices representing the patient's body with the detected tumor shown on figure 3. Figure 4 is the interactive 3D visualization program under ImageJ.

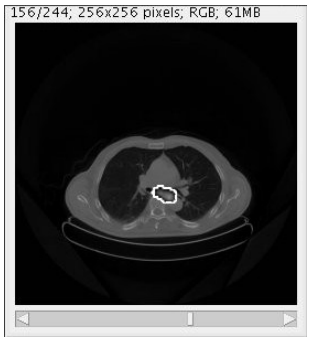

Fig. 3. The resulting combination of stacks i.e. the fusion of segmented PET and CT slices.

Once having combined the three stacks CT, PET and SEGM, the 3D visualization program is based on the volume

viewer plugin [14]. This program allows users to view the resulting stack CT+PET and to interact dynamically with the viewing point.

Fig. 4. Interactive 3D view with tumor detection examples.

Based on segmented tumor images (surface of tumor in images, in pixels), on spatial resolution of PET sensor (1.171875 mm/pixel) and on step between slices (4 mm), an approximation of the volume of the tumor is given to the user of the system. It offers the ability to study the evolution of the tumor between two examinations of the patient and can help a clinician to check if the treatment is adapted to the patient (if the tumor volume decreases in time).

Image	1	2	3	...	8	9	10	11
Pixels	95	147	194	...	200	168	146	131
Volume	111	172	227	...	234	196	171	153

Total tumor pixels : 2110 - Tumor volume (approx.) : 11.59 cm^3. This approximation of the volume of the tumor helps the clinician to check if the given treatment is efficient or not for the patient.

V. CONCLUSION AND FUTURE WORK

A. Conclusion

In this paper, a tumor segmentation and 3D visualization system based on level set method from PET/CT images has been proposed. Segmentation of a concerned region from medical images is a challenging yet unsolved task due to large variations and complexity of the pathological lesions. The proposed segmentation approach has the ability to segment a serial of PET/CT volumes and gives good segmentation results and a good approximation of tumors volumes.

The tool has been developed in Java under ImageJ and thus runs on many architectures. It allows clinicians to interact with a 3D view of the patient's body to observe the tumor. An approximation of the volume of the tumor helps the clinician to follow the evolution of the tumor in time. It makes the study of the evolution of the tumor easier for clinician who can see the result of the treatment on the patient's tumor on a small or long period of time.

B. Future work

The main future direction for this work should be to initialize automatically the level-set algorithm with a pre-detection of the tumor in the slices. This pre-detection could be achieved using classical segmentation techniques. With this future step, our segmentation algorithm would become fully automatic.

Another way of exploration should be to work deeply on level-set parameters λ_1, λ_2, μ and ν in order to improve the quality detection of the pixels of the tumor.

REFERENCES

[1] S. Ruan, C. Jaggi, J. Xue, J. Fadili, and D. Bloyet, "Brain tissue classification of magnetic resonance images using partial volume modeling," *IEEE Trans. on Medical Imaging*, vol. 19, pp. 1179–1187, 2000.

[2] R. Zoroofi, Y. Sato, T. Nishii, N. Sugano, H. Yoshikawa, and S. Tamura, "Automated segmentation of necrotic femoral head from 3d mri data," *Computerized Medical Imaging and Graphics*, vol. 28, pp. 267–278, 2004.

[3] M. Lorenzo-Valdez, G. I. Sanchez-Ortiz, A. G. Elkington, R. H. Mohiaddin, and D. Rueckert, "Segmentation of 4d cardiac mr images using a probabilistic atlas and the em algorithm," *Medical Image Analysis*, vol. 8, pp. 255–265, 2004.

[4] P.-Y. Bondiau, G. Malandain, S. Chanalet, P.-Y. Marcy, J.-L. Habrand, F. Fauchon, P. Paquis, A. Courdi, O. Commowick, I. Rutten, and N. Ayache, "Atlas-based automatic segmentation of mr images: Validation study on brainstem in radiotherapy context," *Int. J. Radiation Oncology Biol. Phys.*, vol. 61, pp. 289–298, 2005.

[5] W. Dou, Q. Liao, S. Ruan, D. Bloyet, J. Constants, and Y. Chen, "Automatic brain tumor extraction using fuzzy information fusion," *Proc. SPIE*, vol. 4875, pp. 604–609, 2002.

[6] J. Sethian, *Level set methods and fast marching methods*. Cambridge University Press, 1999.

[7] C. Xu and al., "Medical image segmentation using deformable models," *Handbook of Medical Imaging*, vol. 2, pp. 129–174, 2000.

[8] A. Farag and al., "3d volume segmentation of mra data sets using level sets," *Academic Radiology*, vol. 11, pp. 419–435, 2004.

[9] K. Xie and al., "Semi-automated brain tumor and edema segmentatio using mri," *European Journal of Radiology*, 2005.

[10] A. Osher and J. Sethian, "Fronts propagating with curvature dependent speed: algorithms based on hamilton-jacobi formulations," *Journal of Computational Physics*, vol. 79, pp. 12–49, 1988.

[11] M. R., S. J.A., and V. B.C., "Shape modeling with front propagation: A level set approach," *IEEE Trans. Pattern Anal. Machine Intell.*, vol. 17, pp. 158–175, 1995.

[12] T. Chan and L. Vese, "Active contours without edges," *IEEE Trans. on Image Processing*, vol. 10, no. 2, pp. 266–277, 2001.

[13] W. Rasband, *ImageJ*, U. S. National Institutes of Health, Bethesda, Maryland, USA, 1997-2007, http://rsb.info.nih.gov/ij/.

[14] K.-U. Barthel, *3-D Volume Viewer plugin for ImageJ*, University of Applied Sciences, Berlin, Germany, 2008, http://www.f4.fhtw-berlin.de/ barthel/.